Journal of Chemical Health Risks

www.jchr.org

JCHR (2025) 15(4), 936-945 | ISSN:2251-6727

Electrochemical And Photocatalytic Studies of Novel Azo Ligand and Their Metal Complexes; Synthesis, Characterization and Biological Evaluation

G.Y. Akarsh[1], G. Krishnamurthy[1*], H.A. Anilkumara[1], N.K. Vasantakumarnaik[1], N. Ranjitha[1], G. Vishnu[2]

[1]Department of P.G. Studies and Research in Chemistry and Industrial Chemistry, Sahyadri Science College, Kuvempu University, Shivamogga - 577203, Karnataka, India.

[2]Department of P.G. Studies and Research in Industrial Chemistry, School of Chemical Sciences, Kuvempu University, Shankaraghatta, 577 451, Karnataka, India.

*Corresponding Author: G. Krishnamurthy

(Received: 16 May 2025 Revised: 20 June 2025 Accepted: 12 July 2025)

KEYWORDS
Azo dye, Metal Complexes, Antidiabetic, Photocatalytic, Cyclic Voltammetry

ABSTRACT:
The Novel Azo Dye ligand, 4-[(2*E*)-3-(6-nitro-1,3-benzothiazol-2-yl)triaz-2-en-1-yl]benzoic acid (NBA) and its Co(II), Ni(II) and Cu(II) complexes have been synthesized. The newly synthesized compounds characterized using physiochemical techniques. XRD pattern indicate crystalline nature of metal complexes. A modified electrode $[Co(NBA)_2(H_2O)_2]$/GCE was prepared by using the synthesized Co(II) complex to assess electrocatalytic properties by cyclic voltammetry (CV) studies. The $[Co(NBA)_2(H_2O)_2]$/GCE found to have excellent electrocatalytic activity with 4.599 µM/L limit of detection (LOD) with a linear range of 10–60 µM/L and $R^2 = 0.9982$ confirming the surface diffusion control of the electrochemical process. The $[Co(NBA)_2(H_2O)_2]$/GCE found efficient in detection of ascorbic acid in different concentrations. Furthermore, the synthesized compounds evaluated for antidiabetic activities exhibiting promising results. The catalytic efficiency of the synthesized metal complexes was assessed through the photodegradation of Methyl Red dye under visible light. The Photocatalytic efficiency of Co(II) and Ni(II) complexes reported to degrade methyl red by 71.58 and 72.13% respectively.

1. Introduction

Azo dyes are synthetic compounds featuring an −N=N− bond, primarily derived from aromatic amine substrates such as nitro and nitroso groups. The azo dye derivatives are significant colorants, which are widely employed in pharmaceuticals, textiles, printing, optics and food processing. The industries availability, affordability, stability and perceived safety of azo dye compounds contribute to their desirability as food additives [1-4]. Azo dye derivatives demonstrate notable antitumor [5], antiulcer [6], antifungal [7], antibacterial [8], anthelmintic [9], anti-inflammatory [10], anticonvulsant [11], antitubercular [12], antidepressant [13], antihypertensive [14], anticoagulant [15], and antiviral [16] activities. Furthermore, azo dye metal chelates are increasingly valued in catalysis, pharmaceuticals and various industrial applications with their transition metal complexes exhibiting biological activity.

Cyclic Voltammetry is a recognized, facile, cost-effective and reliable electrochemical technique for redox studies and elements present in the impure sample detection. This potentiodynamic method investigates the electrochemical properties of analytes in solution or absorbed on the electrode surface [17]. Ascorbic acid (AA) a vital dietary component and potent antioxidant [18] possesses therapeutic benefits for various conditions including fever, fatigue, gum swelling, joint pain and impaired wound healing influences key physiological

Journal of Chemical Health Risks
www.jchr.org
JCHR (2025) 15(4), 936-945 | ISSN:2251-6727

processes. However, its electrochemical activity can interfere with the detection of the other analytes. Ascorbic acid undergo oxidation readily may cause peak overlap with other substances. The oxidation potential and resultant current peak in the cyclic voltammogram are directly correlated with its concentration. Therefore, this method is sensitive to ascorbic acid detection even in the presence of interfering substances.

A number of substituted azo dye ligand and their 3d metal complexes have been synthesized in our laboratory and these complexes used to prepare modified electrode for detecting biologically important molecules and in addition biological activity also been evaluated. In continuation of this, we report here the synthesis of a new azo dye ligand and its transition metal complexes, their biological evaluation, dye degradation and the subsequently detection of ascorbic acid using a $[Co(NBA)_2(H_2O)_2]$/GCE electrode.

2. Experimental Methodology

2.1. Materials and Methods

All Chemicals and solvents used in this study were analytical grade and purchased from Sd-fine and Hi-Media. Ligand and metal complexes melting points were determined using an electrothermal melting point apparatus with a digital thermometer and the values are uncorrected. FT-IR spectra of the synthesized ligand and its metal complexes were recorded on a Shimadzu Spectrometer serial no: A224159 (Made in Japan) in Sahyadri Science College, Shivamogga-577203, Karnataka, India. UV-Vis absorbance was recorded using Systronics UV-Vis Double Beam Spectrophotometer 2206TS in Sahyadri Science College, Shivamogga-577203, Karnataka, India. ^{1}H and ^{13}C NMR spectra of ligand were obtained using a JEOL spectrometer at a frequency of 400 MHz in Mangalore University, Mangalore-574199, Karnataka, India. Mass spectra obtained from Mysore University, Mysore – 570001, Karnataka, India. XRD patterns were obtained using Bruker D8 advance and SEM by Zeiss model-EVO LS 15. Cyclic voltammetry analysis was performed using CH instrument electrochemical analyzer (USA) at Sahyadri Science College, Shivamogga – 577203, Karnataka, India.

2.2. Azo dye ligand synthesis

In a conical flask, solution of 0.002 mol of 2-amino-6-nitrobenzothiazole and 4N HCl dissolved in 10 mL of distilled water. Maintained the reaction mixture in an ice bath with continuous stirring for 2-hours. Simultaneously, 0.002 mol of $NaNO_2$ were dissolved in a separate flask using H_2SO_4 and maintained in an ice bath for 30 minutes. Subsequently, the $NaNO_2$ solution was carefully added to the conical flask with continuous stirring to avoid disruption. Following a 2-hour dissolution of 4-aminobenzoic acid in KOH solution under ice cold conditions, the solution was transferred to a previously prepared solution in a conical flask, stirring continued for an additional hour. Neutralization was achieved using $NaHCO_3$, following which the precipitate was generated, which was filtered, recrystallized and dried. The synthetic pathway is showed in Scheme-1.

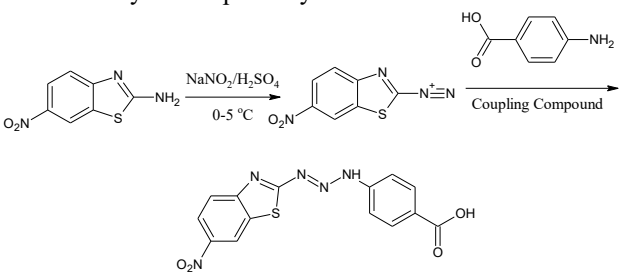

Scheme 1: Synthesized 4-[(1*E*)-3-(6-nitro-1,3-benzothiazol-2-yl)triaz-1-en-1-yl]benzoic acid (NBA)

2.3. Synthesis of Metal Complexes

The synthesized ligand (NBA) (0.002 mol), dissolved in hot absolute ethanol and stirred. The solution of metal chlorides (Co, Ni and Cu) (0.001 mol) in absolute ethanol was prepared and added to the ligand solution. The reaction mixture was refluxed for 5 hours on a water bath. After that the excess solvent was removed by evaporation. The synthesized product was permitted to cool at ambient temperature. The resulting precipitate was subsequently filtered, washed and dried. Scheme 2 illustrates the synthetic pathway and the proposed structure of the metal complexes.

Journal of Chemical Health Risks
www.jchr.org
JCHR (2025) 15(4), 936-945 | ISSN:2251-6727

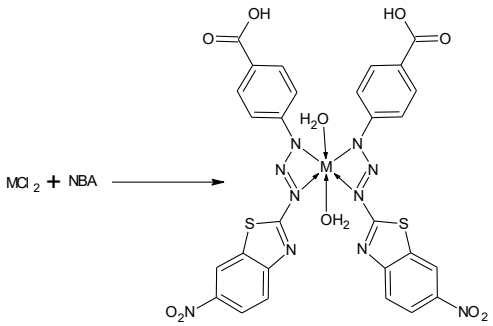

M = Co^{+2}, Ni^{+2} and Cu^{+2}

Scheme 2: Structure of metal Complexes

2.4. Electrochemistry

The electrocatalytic properties of synthesized metal complexes determined by preparing novel modified electrode. A saturated solution of metal complexes in isopropanol was prepared by sonication, was drop-coated onto a glassy carbon electrode (GCE). Cyclic voltammetry employed the GCE as the working electrode, an Ag/AgCl as reference electrode and a platinum wire counter electrode in a phosphate buffer solution was used to study the electrocatalytic activity. Redox reactions of ascorbic acid were induced by cycling the potential applied to the working electrode and the resulting current response correlated to ascorbic acid concentration via peak currents and calibration curves enabled quantitative analysis. This method provides rapid sensitive ascorbic acid detection with broad applicability [19-20].

2.4. Photocatalytic Activity

Methyl red (MR) degradation under natural sunlight was used to evaluate photocatalytic activity. A 50 mg photocatalyst sample was dispersed in 100 mL of aqueous MR solution. Prior to irradiation, the suspensions were magnetically stirred in the dark for 15 minutes to establish MR adsorption-desorption equilibrium. At predetermined intervals, 3mL aliquots were withdrawn, centrifuged to remove particles and MR concentration was determined by absorbance measurement observed at the characteristic wavelength using Systronics 2206TS UV-Vis double Beam Spectrophotometer [21-22].

2.5. Antidiabetic activity

α-Amylase inhibitory activity

α-Amylase inhibition assays were conducted according to the method detailed in Gharge et al., 2024 [23]. Porcine pancreatic α-amylase (1 U/mL; SRL, Bangalore, India) was prepared in 0.1 M phosphate-buffered saline (pH 6.9) at a concentration of 100 µL. Enzymes sample at concentrations range from 0 to 100 µg/mL underwent a 10-minute pre-incubation at 37 °C. The reaction commenced upon the addition of 0.1% starch substrate to the incubation mixture. Following 10-minute incubation period, the reaction mixture was quenched by the addition of 250 µL of dinitrosalicylic acid (DNS) reagent (1% 3,5-dinitrosalicylic acid, 0.2% phenol, 0.05% Na_2SO_3 and 1% NaOH in aqueous solution). The reaction was quenched by maintaining the reaction mixture in a boiling water bath for 10 minutes. Subsequently, 250 µL of a 40% potassium sodium tartrate solution was introduced. Following cooling to ambient temperature in a cold-water bath, absorbance was measured at 540 nm. The percentage inhibition was determined using the formula (OD of blank – OD of test/OD of blank) × 100, and the results were expressed as IC_{50} values with acarbose serving as a positive control.

α-Glucosidase inhibitory activity

The α-glucoside inhibitory activity of the samples using the methodology [24]. Specifically, 50µL of 1 U/mL yeast α-glucoside (SRL, Bangalore, India) in 50 mM phosphate buffer (pH 6.9) was pre-incubated with varying sample concentrations (0-100 µg/mL) for 10 minutes at 37 °C. The reaction was initiated by adding 50 µL of 5 mM p-nitrophenyl-α-D-glucopyranoside in phosphate buffer, incubated for 30 minutes at 37 °C and subsequently quenched with 1 M Na_2CO_3. Absorbance was measured at 405 nm. Inhibition percentage was determined using the formula (OD of blank – OD of test/OD of Blank) ×100 and results are reported as IC_{50} values with acarbose serving as a positive control.

3. Results and Discussion

3.1. Chemistry

The novel azo dye ligand and its metal complexes exhibited stability at ambient temperature and solubility in ethanol, methanol, DMF, chloroform and DMSO. Elemental analysis data corroborated calculated values, as presented in Table 1.

Journal of Chemical Health Risks
www.jchr.org
JCHR (2025) 15(4), 936-945 | ISSN:2251-6727

Table 1 Physical properties and analytical data of the NBA and its metal complexes

Compounds	Mol.Wt	Calculated CHN values in (%)				Melting Point (°C)
		M	C	H	N	
NBA	344.04	-	48.98 (48.67)	2.64 (2.47)	20.40 (20.19)	183
$[Co(NBA)_2(H_2O)_2]$	778.46	7.55 (7.43)	43.14 (42.89)	2.59 (2.47)	17.97 (17.86)	261
$[Ni(NBA)_2(H_2O)_2]$	778.88	7.53 (7.45)	43.09 (42.57)	2.57 (2.43)	17.91 (17.79)	257
$[Cu(NBA)_2(H_2O)_2]$	783.28	8.10 (7.95)	42.58 (42.37)	2.47 (2.34)	17.66 (17.53)	263

3.2. ^{1}H NMR Spectral Studies

The aromatic protons in the ^{1}H NMR spectrum of NBA appeared as multiplets in the region 7.6 – 8.5 ppm. A singlet observed at 4.9 ppm, corresponding to the NH proton. An additional sharp singlet at 12.8 ppm is an indicative of an aromatic OH as showed in the spectrum Figure 1.

The ^{13}C NMR spectrum of the NBA exhibited fourteen distinct carbon chemical environments, resonating between 100 and 171 ppm. The C=O group exhibited a resonance at 171.81 ppm, while the remaining benzene ring carbons resonated between 112 and 140 ppm. Literature data corroborates the proposed molecular structure, with the ^{1}H and ^{13}C NMR spectra showing excellent agreement. The ^{13}C NMR spectral data are showed in Figure 2.

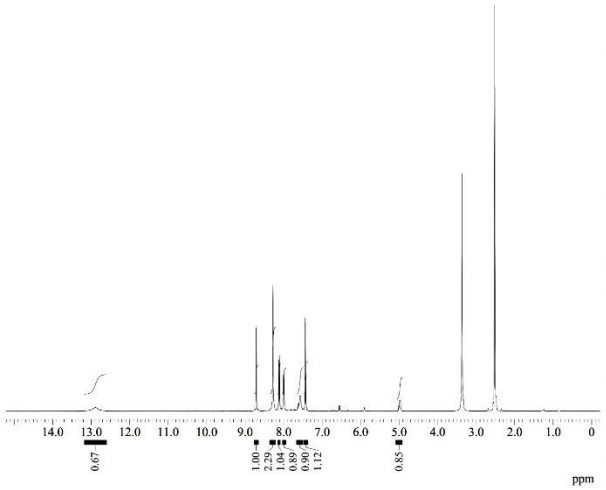

Figure 1 ^{1}H NMR spectrum of NBA

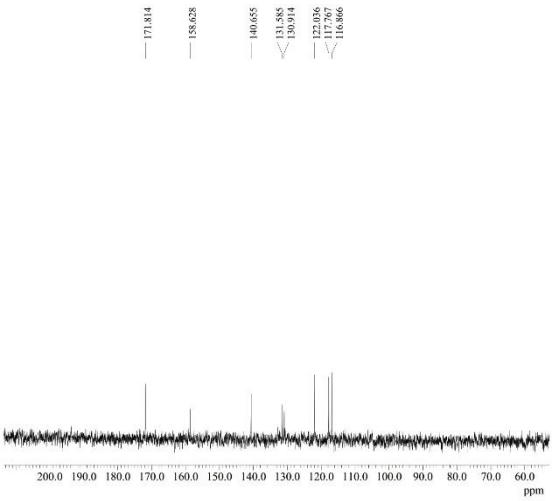

Figure 2 ^{13}C Spectrum of NBA

3.3. Mass Spectral Studies

Mass spectral analysis of the synthesized ligand and its metal complexes was performed. The molecular ion peak in the ligand (NBA) mass spectrum, observed at m/z 344.04 (cal. 343.41) confirms the proposed molecular formula showed in Figure 3. Molecular ion peaks for the Co(II), Ni(II) and Cu(II) complexes were detected at m/z 778.46 (cal. 779.53), 778.88 (cal. 779.34) and 783.28 (cal. 784.17) respectively supporting the proposed 1:2 (M:L) stoichiometric ratio. Observed spectral data are consistent with the proposed molecular structures.

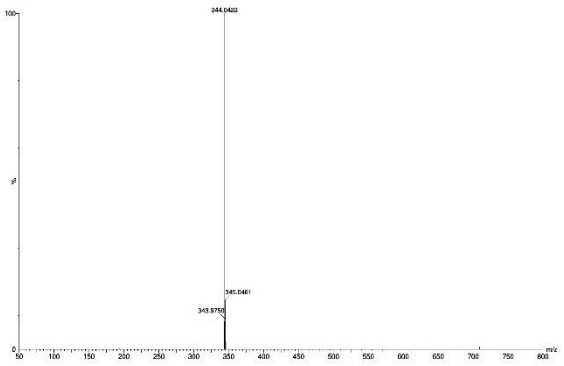

Figure 3 Mass spectrum of NBA

3.4. IR Spectral Studies

Infrared spectroscopy proved essential in identifying the functional groups of the synthesized ligand (NBA) and its metal complexes. The infrared spectra of NBA and its metal complexes recorded using KBr pellets in the 4000 – 350 cm^{-1} wavelength range are presented in Figure 4.

Journal of Chemical Health Risks
www.jchr.org
JCHR (2025) 15(4), 936-945 | ISSN:2251-6727

The data placed in Table 2 indicate the – OH stretching vibration at 3430 cm^{-1}. The –OH stretching bands appeared at nearly identical regions across all complexes with minor shifts 20 – 30 cm^{-1} to higher frequencies. The –N=N– stretching was observed around 2027 cm^{-1} exhibiting similar minor shifts of 30 – 40 cm^{-1} to higher frequencies across all complexes. The C=O stretching remained at approximately 1649 cm^{-1} in all complexes showing no significant shifts. The involvement of the ligand and metal ion via –N=N– group in complex formation is supported by appearing new bands in the region 427 – 470 cm^{-1} which are assigned to M–N vibration modes.

Table 2 FTIR spectral data (cm^{-1}) of NBA and its metal complexes

Compounds	ν (OH)	ν(N=N)	ν(C=O)	ν (M–N)
NBA	3430	2027	1649	-
$[Co(NBA)_2(H_2O)_2]$	3467	2048	1645	470
$[Ni(NBA)_2(H_2O)_2]$	3452	2041	1641	441
$[Cu(NBA)_2(H_2O)_2]$	3445	2034	1643	427

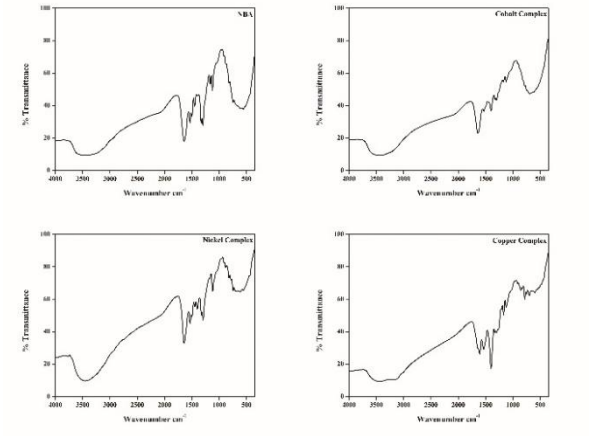

Figure 4 FT-IR spectra of NBA and its metal complexes

3.5. Electronic Spectral and Magnetic moment analysis

The electronic spectra of the synthesized Schiff base ligand and its metal complexes represented in Figure 5. With the numerical values detailed in Table 3. The NBA compound exhibits an absorption band at 26,666 cm^{-1} attributed to charge transfer transition. The $[Co(NBA)_2(H_2O)_2]$ complex displays two bands at 16,260 cm^{-1} and 14,836 cm^{-1} corresponding to $^4T_{1g}(F)\rightarrow{}^4T_{1g}(F)$ and $^4T_{1g}(F)\rightarrow{}^4T_{2g}(F)$ transitions respectively. The magnetic moment of 3.80 BM and electronic transition suggest an octahedral geometry. The $[Ni(NBA)_2(H_2O)_2]$ complex exhibits transitions at 14,306 cm^{-1}, 13,368 cm^{-1} and 10,499 cm^{-1} assigned to $^3A_2g(F)\rightarrow{}^3T_1g(P)$, $^3A_{2g}(F)\rightarrow{}^3T_{1g}(F)$ and $^3A_{2g}(F)\rightarrow{}^3T_{2g}(F)$ transition respectively. The observed magnetic moment of 2.75 BM indicated an octahedral geometry. The $[Cu(NBA)_2(H_2O)_2]$ complex shows a broad band at 10,030 cm^{-1} corresponds to $^2E_g\rightarrow{}^2T_{2g}$ consistent with an octahedral geometry and a magnetic moment of 1.78 BM.

Table 3 Electronic absorption spectral bands

Compounds	λ (nm)	Transitions (cm^{-1})	Magnetic Moment (BM)
NBA	374	26,666	-
$[Co(NBA)_2(H_2O)_2]$	615 674	16,260 14,836	3.80
$[Ni(NBA)_2(H_2O)_2]$	699 748 957	14,306 13,368 10,449	2.75
$[Cu(NBA)_2(H_2O)_2]$	997	10,030	1.78

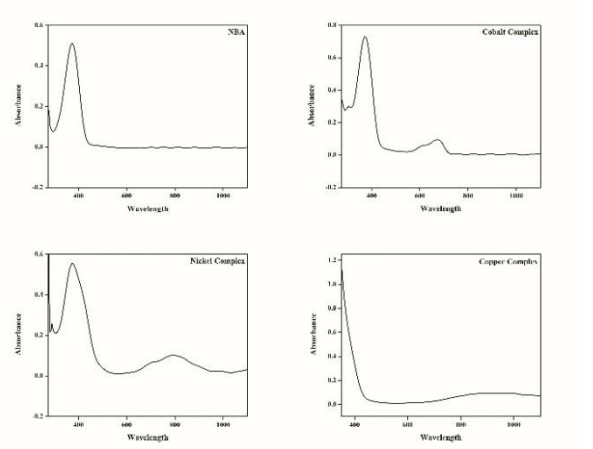

Figure 5 Electronic absorption spectra of NBA and its metal complexes

3.6. X-ray diffraction studies

X-ray diffraction patterns of the metal complexes were recorded over a 2θ range of 0-80° as shown in Figure 6. The calculated lattice parameter a=b=c of Co(II) 16.44, Ni(II) 15.23 and Cu(II) 16.77. The sharp peaks observed indicates the crystalline nature of the metal complexes. [25].

Journal of Chemical Health Risks
www.jchr.org
JCHR (2025) 15(4), 936-945 | ISSN:2251-6727

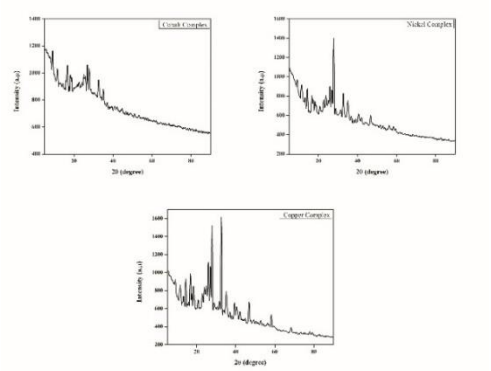

Figure 6 Power XRD of NBA and its metal complexes

4. Electrochemical Studies

4.1 Electrochemical detection of different electrodes

Electrochemical properties of the synthesized compounds have been studied by determining their electrochemical sensing ability. For which a modified electrode is prepared by dissolving synthesized compounds with isopropanol and coated a layer on the surface of glassy carbon electrode (GCE). The redox potential obtained by modified electrode was compared with redox potential of GCE. The solution of ascorbic acid (AA) in pH 7 of phosphate buffer solution was prepared in which both GCE and modified electrode placed and electrochemical detection was determined. Among the synthesized metal complexes $[Co(NBA)_2(H_2O)_2]$/GCE found more suitable, therefore modified electrode $[Co(NBA)_2(H_2O)_2]$/GCE has been used for further studies. The results in a significantly increased peak current as illustrated in Figure 7.

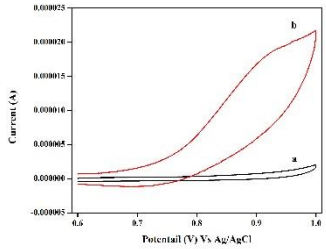

Figure 7 Cyclic Voltammograms of (a) bare electrode and (b) $[Co(NBA)_2(H_2O)_2]$/GCE with AA 10 µM/L at a scan rate = 50 mV/s

4.2. Electrochemical detection of Ascorbic Acid at different concentration

Cyclic Voltammetry (CV) was used to determine Ascorbic acid (AA) concentration in pH 7 PBS using a $[Co(NBA)_2(H_2O)_2]$/GCE. Figure 8. Show the CV of the modified GCE with and without AA recorded at a 50 mV/s scan rate. The bare GCE has no characteristic peaks between 0.6 and 1.0 V in PBS. However, the $[Co(NBA)_2(H_2O)_2]$/GCE exhibited a well-defined peak upon AA addition. The AA oxidation peak current increased significantly at $[Co(NBA)_2(H_2O)_2]$/GCE demonstrating superior electrocatalytic activity for AA oxidation compared to the unmodified GCE. Analytical parameters for AA detection using the modified GCE include a 4.599 µM/L detection limit. The linear regression equation is $y = 6.466\times10^{-8}$ (AA) + 1.0765×10^{-5} (R^2 = 0.9982). Each calibration graph data point represents the mean of independent measurements [26].

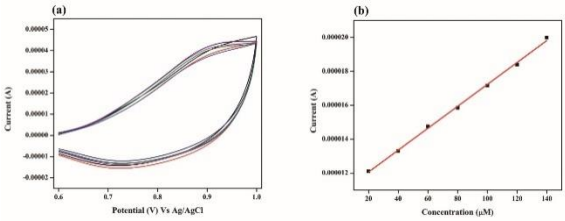

Figure 8 Cyclic Voltammetry of $[Co(NBA)_2(H_2O)_2]$/GCE was performed at (a) varying concentrations from 10 to 60 µM/L and (b) a linear correlation between peak current and concentration was established in PBS (pH 7) at a scan rate of 50 mV/s

4.3. Different Scan rate of Ascorbic acid

Cyclic Voltammetry investigated the impact of scan rate on the peak currents of AA using $[Co(NBA)_2(H_2O)_2]$/GCE. Measurements were performed at a scan rate from 0.01 to 0.09 V/s in pH 7 PBS as illustrated in Figure 9. The peak current demonstrates a linear correlation with R^2 = 0.9958 confirming the surface diffusion control of the electrochemical process [27].

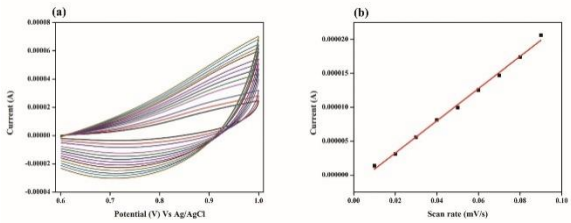

Fig. 9. Ascorbic acid concentrations were varied; Scan rates ranged from 0.01 to 0.09 mV/s (a) A calibration graph depicting the square root of the scan rate vs peak current is shown in the inset and (b) presents a linear

Journal of Chemical Health Risks
www.jchr.org
JCHR (2025) 15(4), 936-945 | ISSN:2251-6727

graph of peak current vs scan rate for the modified electrode.

Table 4 Comparison of present work with literature for the detection of ascorbic acid

Electrodes	Detection methods	Linear range (µM)	LOD (µM/L)	Reference
Gr/CuPc/PANI	CV	0.5 - 0.12	0.06	28
GCE/MWCNT/PdPc	CV	0.3 - 2.4	1.0	29
Azo-bridzed-CuPc polymer/GCE	CV	5 - 120	1.66	30
$Co(NBA)_2(H_2O)_2$]/GCE	CV	10 - 60	4.599	This Work

5. Photocatalytic Studies

Photocatalytic activity of synthesized Co(II), N(II) and Cu(II) metal complexes was assessed via irradiation under natural sunlight. Graphically Figure 10. depicts methyl red dye absorption maxima observed at 363.43, 361.43 and 360.94 nm for synthesized Co(II), Ni(II) and Cu(II) complexes respectively. Increased irradiation time correlated with decreased methyl red absorbance in the presence of the synthesized metal complexes. Co(II), Ni(II) and Cu(II) complexes respectively exhibited 71.58, 72.13 and 59.19% of degradation efficiency against methyl red respectively. Therefore, Co(II) and Ni(II) complexes demonstrated superior photodegradation performance when compared to Cu(II) complex [31].

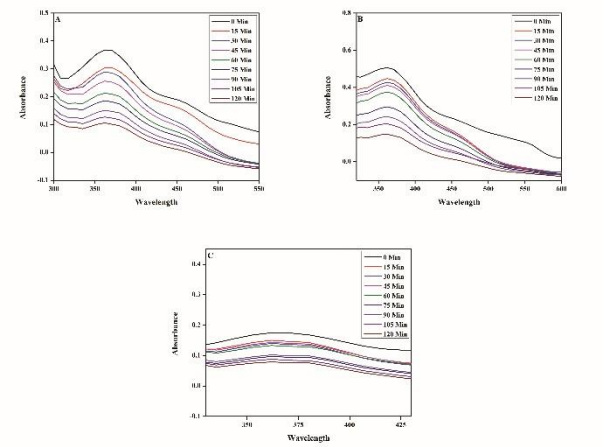

Figure 10 Photodegradation of methyl red with Co(II), Ni(II) and Cu(II) complexes

6. Antidiabetic activity

The antidiabetic activity of the synthesized ligand and its metal complexes was determined using the IC_{50} method as described in the procedure section. Alpha-amylase and alpha-glucosidase enzyme activity was screened and the results are tabulated in Table 5 and comparatively illustrated in Figure 11. The $[Co(NBA)_2(H_2O)_2]$ and $[Ni(NBA)_2(H_2O)_2]$ complexes exhibited promising activity compared to the uncoordinated ligand and the standard [32].

Table 5 α-Amylase inhibition property of Samples in IC_{50} (µg/mL)

Sample Name	α-Amylase inhibition (IC_{50} µg/mL)	α-Glucosidase inhibition (IC_{50} µg/mL)
NBA	105.19	59.59
$[Co(NBA)_2(H_2O)_2]$	147.75	91.92
$[Ni(NBA)_2(H_2O)_2]$	118.24	90.70
$[Cu(NBA)_2(H_2O)_2]$	105.19	68.17
Std (Acarbose)	32.35	26.70

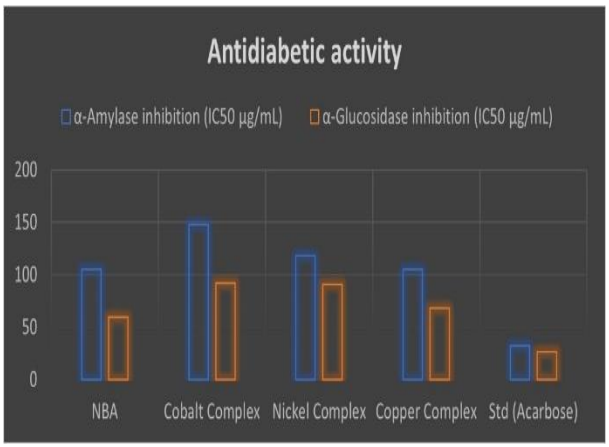

Figure 11 Antifungal activity of NBA and its metal complexes

7. Conclusion

The study emphasis on synthesis and characterization of the biologically active Co(II), Ni(II) and Cu(II) complexes of the novel 4-[(2*E*)-3-(6-nitro-1,3-benzothiazol-2-yl)triaz-2-en-1-yl]benzoic acid (NBA). The ligand acts as bidentate and the spectral study show an octahedral geometry for metal complexes. $[Co(NBA)_2(H_2O)_2]$/GCE prepared by incorporating the synthesized metal complexes exhibited excellent electrocatalytic activity at varying concentrations and has a low limit of detection (LOD) of 4.599 µM/L with $R^2 = 0.9982$. The photocatalytic degradation efficiency of the synthesized metal complexes evaluated where methyl

Journal of Chemical Health Risks

www.jchr.org

JCHR (2025) 15(4), 936-945 | ISSN:2251-6727

red (MR) found to undergo most effective degradation when compared to other dyes. Results also indicate that the Co(II) and Ni(II) complexes exhibited a 71.58 and 72.13% degradation efficiency respectively. In addition, the ligand showed significant antidiabetic activity. However, its metal complexes exhibited pronounced antidiabetic activity.

References

1. N. Ranjitha, G. Krishanamurthy, M.N. Manjunath, H. S. Bhojya Naik, Malathesh Pari, N. K. Vasanthkumarnaik, J. Lakshmikantha, K. Pradeep, Electrochemical determination of glucose and H_2O_2 using Co(II), Ni(II), Cu(II) complexes of novel 2-(1,3-benzothiazol-2-ylamino)-N-(5-chloro-2-hydroxyphenyl)acetamide: Synthesis, structural characterisation, antimicrobial, anticancer activity and docking studies, J. Mol. Struct. 1274 (2023) 134483.
2. N. Venugopal, G. Krishnamurthy, H. S. Bhojya Naik, P. Muruli Krishna, Synthesis, spectral characterization and biological studies of Cu (II), Co (II) and Ni (II) complexes of azo dye ligand containing 4–amino antipyrine moiety, J. Mol. Struct. 1183 (2019) 37-51.
3. N. Sunil Kumar, G. Krishnamurthy, D. Yadav Bodke, H. Vikas Malojirao, T. R. Ravikumar Naik, Shivananda Kandagalla, B. T. Prabhakar, Synthesis, characterization and tumor inhibitory activity of a novel Pd(II) complex derived from methanethiol-bridged (2-((1*H*-benzo[*d*]imidazol-2-yl)methylthio)-1*H*-benzo[*d*]imidazol-6-yl)(phenyl)methanone, New J. Chem. 43 (2019) 790-806.
4. N. Sunil Kumar, G. Krishnamurthy, Madhusudana somegowda, Maltesh Pari, T. R. Ravikumar Naik, K. S. Jithendra Kumar, Satish Naik, ShivanandaKandagalla, Nagaraja Naik, Synthesis, characterization, electrochemistry, biological and molecular docking studies of the novel Co(II), Ni(II) and Cu(II) complexes derived from methanethiol bridged (2-((1H-benzo[d]imidazol-2-yl)methylthio)-1H-benzo[d]imidazol-6-yl)(phenyl)methanone, J.Mol.Struct. 1220 (2020) 128586.
5. Asal Jalal Abadi, Sepideh Mirzaei, Mahmood Khaksary Mahabady, Farid Hashemi, Amirhossein Zabolian, Fardin Hashemi, Pourya Raee, Shahin Aghamiri, Milad Ashrafizadeh, Amir Reza Aref, R. Michael. Hamblin, Kiavash Hushmandi, Ali Zarrabi, Gautam Sethi, Curcumin and its derivatives in cancer therapy: Potentiating antitumor activity of cisplatin and reducing side effects, Phytother.Res. 36 (2021) 189-213.
6. P. Senthil Kumar, G. Janet Joshiba, C. Carolin Femina, P. Varshini, S. Priyadharshini, M. A. Karthik, R. Jothirani, A critical review on recent developments in the low-cost adsorption of dyes from wastewater, Desalin water treat 172 (2019) 395-416.
7. L. Cottet, C. A. P. Almeida, N. Naidek, M. F. Viante, M. C. Lopes, N. A. Debacher, Adsorption characteristics of montmorillonite clay modified with iron oxide with respect to methylene blue in aqueous media, Appl. Clay Sci. 95 (2014) 25-31.
8. J. Khalid AL-Adilee, K. Ahmed Abass, M. Taher, Synthesis of some transition metal complexes with new heterocyclic thiazolyl azo dye and their uses as sensitizers in photo reactions, J.Mol.Struct 1108 (2016) 378-397.
9. Zabiulla, Salma Kouser, Mahima Joythi , A. Bushra Begum, M.S. Asha, Fares Hezam Al-Ostoot, D. P. Lakshmeesha, Ramith Ramu, Shaukath Ara Khanum, Molecular docking, synthesis and antimicrobial evaluation of metal complexes with Schiff base, Results Chem. 5 (2016) 100650.
10. A.G. Prashantha, J. Keshavayya and R. A. Shoukat Ali, Synthesis and studies on novel toluic acid-based azo dyes, RJC 14 (2021) 1635-1642.
11. Jakob Avi Shimshoni, Stefan Soback, Olga Cuneah, Alan Shlosberg, Malka Britzi, New validated multiresidue analysis of six 4-hydroxy-coumarin anticoagulant rodenticides in hen eggs, 25 J. Vet. Diagn. (2013) 736-743.
12. Chita Ranjan Sahoo, Jyotirmaya Sahoo, Monalisa Mahapatra, Debananda Lenka, Pratap Kumar Sahu, Budheswar Dehury, Rabindra Nath Padhy, Sudhir Kumar Paidesetty. Coumarin derivatives as promising antibacterial agent(s), Arab. J. Chem. 14 (2021) 102922.
13. Rahman Abdizadeh, Farzin Hadizadeh, Tooba Abdizadeh. In silico analysis and identification of antiviral coumarin derivatives against 3-chymotrypsin-like main protease of the novel

Journal of Chemical Health Risks

www.jchr.org

JCHR (2025) 15(4), 936-945 | ISSN:2251-6727

coronavirus SARS-CoV-2, Mol. Divers. 26 (2022) 1053-1076.

14. Mohd Zaheen Hassan, Hasnah Osman, Mohamed Ashraf Ali, Mohamed Jawed Ahsan, Therapeutic potential of coumarins as antiviral agents,Eur. J. Med. Chem. 123 (2016) 236-255.
15. Saeed Emami, Sakineh Dadashpour, Current developments of coumarin-based anti-cancer agents in medicinal chemistry, Eur. J. Med Chem.102 (2015) 611-630.
16. M. Juri Timonen, M. Riina Nieminen, Outi Sareila, Antonis Goulas, J. Lauri Moilanen, Matti Haukka, Pirjo Vainiotalo, Eeva Moilanen, H. Paula Aulaskari, Synthesis and anti-inflammatory effects of a series of novel 7-hydroxycoumarin derivatives, Eur. J. Med. Chem. 46 (2011) 3845-3850.
17. Xiaohua Liang, Peng Song, Zhan Wang, Zhenping Qin, Hongxia Guo, Insights into kinetics extraction of the homogeneous electrocatalytic reaction between TMPD and ascorbic acid by cyclic voltammetry, J. Electroanal. Chem. 904 (2022) 115948.
18. Sona Skrovankova, Jiri Mlcek, Jiri Sochor, Mojmir Baron, Jindrich Kynicky, Tunde Jurikov, Determination of Ascorbic Acid by Electrochemical Techniques and other Methods, Int. J. Electrochem. Sci. 10 (2015) 2421-2431.
19. Arash Babakhanian, Samineh Kaki, Mahtab Ahma di, Hosna Ehzari, and Afshin Pashabadi. Biosens.Bioelectron. 60 (2014) 185-190.
20. N. Ranjitha, G. Krishnamurthy, H.S. Bhojya Naik, Maltesh Pari, Lubna Afroz, K.R. Sumadevi, M.N. Manjunath, Structural elucidation, voltammetric detection of dopamine, molecular docking and biological inspection of novel 4-aminoantipyrine derived Schiff bases in Co (II), Ni (II) and Cu (II) complexes, Inorganica Chim. Acta. 543 (2022) 121191.
21. Keiichi Tanaka, Kanjana Padermpole, Teruaki Hisa naga, Photocatalytic degradation of commercial azo dyes, Water Res. 34 (2000) 327-333.
22. Ammar Houas, Hinda Lachheb, Mohamed Ksibi, E limame Elaloui, Chantal Guillard, Jean-Marie Herrmann, Photocatalytic degradation pathway of methylene blue in water, Appl. Catal. 31 (2001) 145-157.
23. Shankar Gharge, Shankar G. Alegaon , Shriram D. Ranade, N.A. Khatib, Rohini S. Kavalapure, B.R. Prashantha Kumar, Vinod D, Nandkishor B. Bavage, Design, synthesis of new 2,4-thiazolidinediones: *In-silico*, *in-vivo* anti-diabetic and anti-inflammatory evaluation, Eur. J. Med. Chem. Rep. 11 (2024) 100151.
24. Mei Feng, Bingwen Liang, Jinping Sun, Xiaofeng Min, ShaoHua Wang, Yujing Lu, Xuetao Xu, Synthesis, anti-α-glucosidase activity, inhibition interaction, and anti-diabetic activity of novel cryptolepine derivatives, J. Mol. Struct. 1310 (2024) 138311.
25. Lawrence Kumar, Pawan Kumar, Amarendra Narayan, Manoranjan Kar, Rietveld analysis of XRD patterns of different sizes of nanocrystalline cobalt ferrite, Int. Nano Lett. 3 (2013) 1-12.
26. D. Sangamithirai, S. Munusamy, V. Narayanan, A. Stephen, A voltammetric biosensor based on poly(o-methoxyaniline)-gold nanocomposite modified electrode for the simultaneous determination of dopamine and folic acid, Mater.Sci.Eng.C. 91 (2018) 512-523,
27. H.A. Anilkumara, G. Krishnamurthy, M. N. Manjunatha, Prabhakar Chavan, Malathesh Pari, N Ranjitha, Fasiulla Khan, Synthesis, Structural Determination, Electrochemical Investigation of Metal Complexes of Novel 4-[3-Hydroxypyridin-2-yl)diazenyl]-5-methyl-2-phenyl-2,4-dihydro-3H-pyrazol-3-one; Biological Evaluations, ABEC. 16 (2023) 537-558.
28. S. Pakapongpan, J. P. Mensing, D. Phokharatkul, T. Lomas, and A. Tuantranont, Electrochim. Acta 133 (2014) 294.
29. N. Manjunatha, A. Shambulinga, D. Imdadulla, C. P. Keshavananda Prabhu, and K. S. Lokesh, Microchem. J. 143 (2018) 82.
30. Malathesh Pari, Mounesh, Bhvimanesanna Jilani and K. R. Venugopala Reddy Anal. Bioanal. Electrochem., Vol. 11, No. 4, 2019, 460-483.
31. Vishnu G, Simranjeet Singh, T.S. Sunil Kumar Naik, R Viswanath, Praveen C. Ramamurthy, Pooja Bhadrecha, HS Bhojya Naik, Joginder Singh, Nadeem A. Khan, Sasan Zahmatkesh, Photodegradation of

methylene blue dye using light driven photocatalyst-green cobalt doped cadmium ferrite nanoparticles as antibacterial agents, J.Clen.Pod. 404 (2023) 136977,

32. Ebru Deveci, Fatih Çayan, Gülsen Tel-Çayan, Mehmet Emin Duru, Inhibitory activities of medicinal mushrooms on α-amylase and α-glucosidase-enzymes related to type 2 diabetes, S AFR J BOT. 137 (2021) 19-23.